Unconventional transition to topological superconductivity in a self-organized magnetic ladder

Tadeusz DOMAŃSKI

M. Curie-Skłodowska University (Lublin, Poland)

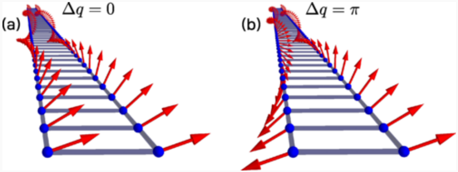

Physics of Magnetism (Poznań) **30 June 2021**

COAUTHORS

⇒ **Maciek Maśka**

(Technical University, Wrocław)

⇒ **Nick Sedlmayr**

(M. Curie-Skłodowska University, Lublin)

⇒ **Aksel Kobiałka**

(M. Curie-Skłodowska University, Lublin)

Bulk superconductors

Perfect conductor

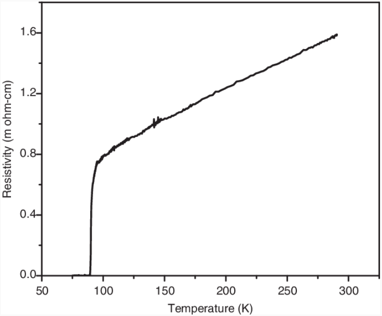

SUPERCONDUCTIVITY

Perfect conductor

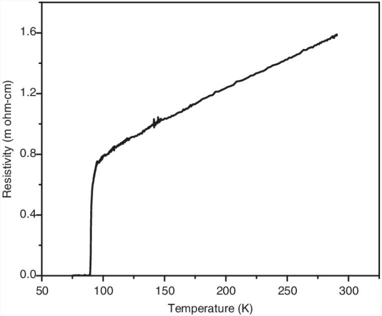

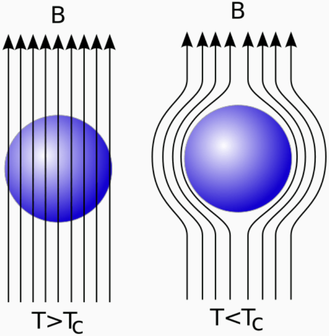

Perfect diamagnet

ELECTRON PAIRING

BCS (non-Fermi liquid) ground state :

$$|\mathbf{BCS}\rangle = \prod_{k} \left(u_k + v_k \; \hat{c}^{\dagger}_{k\uparrow} \, \hat{c}^{\dagger}_{-k\downarrow} \right) \; |\mathbf{vacuum}\rangle$$

BCS (non-Fermi liquid) ground state :

$$|\mathbf{BCS}\rangle = \prod_k \left(u_k + v_k \; \hat{c}^\dagger_{k\uparrow} \; \hat{c}^\dagger_{-k\downarrow} \right) \; |\mathbf{vacuum}\rangle$$

$|v_k|^2 \Rightarrow$ **probablity of occupied momenta** $(k\uparrow, -k\downarrow)$

BCS (non-Fermi liquid) ground state :

$$|\mathbf{BCS}\rangle = \prod_k \left(u_k + v_k\ \hat{c}^\dagger_{k\uparrow}\ \hat{c}^\dagger_{-k\downarrow}\right)\ |\mathbf{vacuum}\rangle$$

$|v_k|^2 \Rightarrow$ **probablity of occupied momenta** $(k\uparrow, -k\downarrow)$

$|u_k|^2 \Rightarrow$ **probablity of unoccupied momenta** $(k\uparrow, -k\downarrow)$

BCS (non-Fermi liquid) ground state :

$$|\mathbf{BCS}\rangle = \prod_k \left(u_k + v_k \; \hat{c}^\dagger_{k\uparrow} \, \hat{c}^\dagger_{-k\downarrow} \right) \; |\mathbf{vacuum}\rangle$$

$|v_k|^2 \Rightarrow$ **probablity of occupied momenta** $(k\uparrow, -k\downarrow)$

$|u_k|^2 \Rightarrow$ **probablity of unoccupied momenta** $(k\uparrow, -k\downarrow)$

quasiparticle = coherent superposition of a particle and hole

$$\begin{aligned} \hat{\gamma}_{k\uparrow} &= u_k \hat{c}_{k\uparrow} + v_k \hat{c}^\dagger_{-k\downarrow} \\ \hat{\gamma}^\dagger_{-k\downarrow} &= -v_k \hat{c}_{k\uparrow} + u_k \hat{c}^\dagger_{-k\downarrow} \end{aligned}$$

ELECTRON PAIRING

BCS (non-Fermi liquid) ground state :

$$|\mathrm{BCS}\rangle = \prod_k \left(u_k + v_k \; \hat{c}^\dagger_{k\uparrow} \; \hat{c}^\dagger_{-k\downarrow} \right) \; |\mathrm{vacuum}\rangle$$

$|v_k|^2 \Rightarrow$ **probablity of occupied momenta** $(k\uparrow, -k\downarrow)$

$|u_k|^2 \Rightarrow$ **probablity of unoccupied momenta** $(k\uparrow, -k\downarrow)$

quasiparticle = coherent superposition of a particle and hole

$$\begin{aligned} \hat{\gamma}_{k\uparrow} &= u_k \hat{c}_{k\uparrow} + v_k \hat{c}^\dagger_{-k\downarrow} \\ \hat{\gamma}^\dagger_{-k\downarrow} &= -v_k \hat{c}_{k\uparrow} + u_k \hat{c}^\dagger_{-k\downarrow} \end{aligned}$$

Charge is conserved modulo-2e due to Bose-Einstein condensation of Cooper pairs

$$\begin{aligned} \hat{\gamma}_{k\uparrow} &= u_k \hat{c}_{k\uparrow} + \tilde{v}_k \; \hat{b}_{q=0} \hat{c}^\dagger_{-k\downarrow} \\ \hat{\gamma}^\dagger_{-k\downarrow} &= -\tilde{v}_k \; \hat{b}^\dagger_{q=0} \; \hat{c}_{k\uparrow} + u_k \hat{c}^\dagger_{-k\downarrow} \end{aligned}$$

BOGOLIUBOV QUASIPARTICLES

Quasiparticle spectrum of conventional superconductors consists of two Bogoliubov (p/h) branches, gaped around E_F

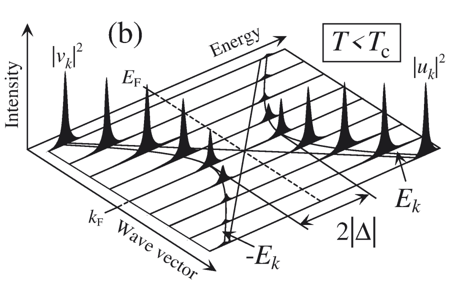

Quasiparticle spectrum of conventional superconductors consists of two Bogoliubov (p/h) branches, gaped around E_F

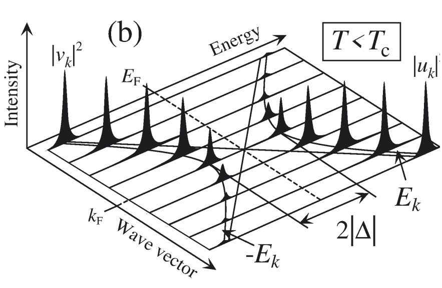

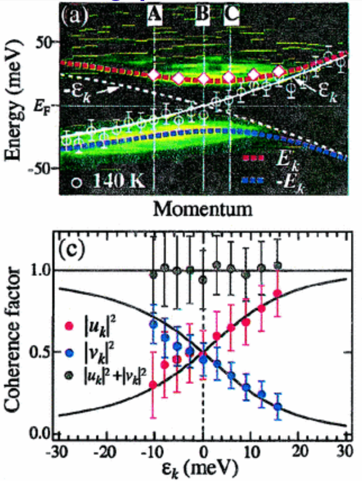

H. Matsui et al, Phys. Rev. Lett. 90, 217002 (2003).

PARTICLE VS HOLE

In all superconductors the particle and hole degrees of freedom are mixed with one another

PARTICLE VS HOLE

In all superconductors the particle and hole degrees of freedom are mixed with one another (this is particularly evident near E_F)

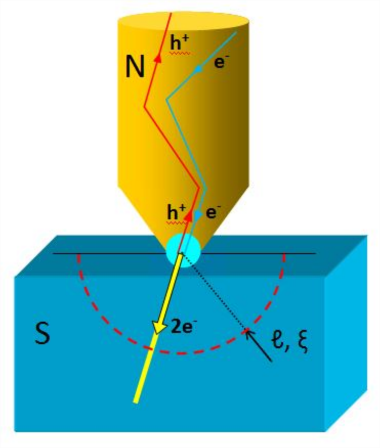

Magnetic impurities in superconductors

IN-GAP STATES OF MAGNETIC IMPURITIES

Magnetic impurities existing in bulk superconductors are pair-breakers.

IN-GAP STATES OF MAGNETIC IMPURITIES

Magnetic impurities existing in bulk superconductors are pair-breakers.

Typical spectrum of a single impurity in s-wave superconductor:

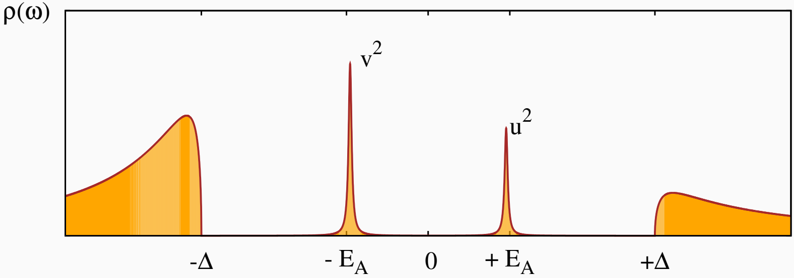

Bound states appearing in the subgap region $E \in \langle -\mathbf{\Delta}, \mathbf{\Delta} \rangle$

IN-GAP STATES OF MAGNETIC IMPURITIES

Magnetic impurities existing in bulk superconductors are pair-breakers.

Typical spectrum of a single impurity in s-wave superconductor:

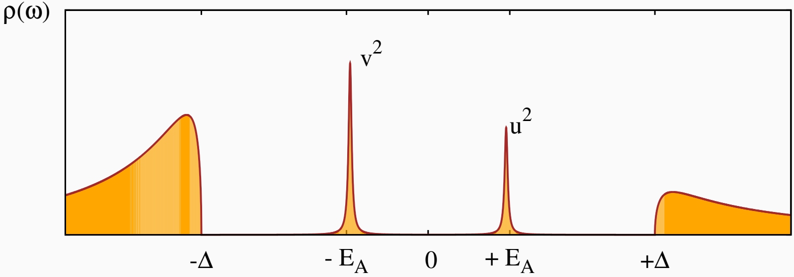

Bound states appearing in the subgap region $E \in \langle -\Delta, \Delta \rangle$

are dubbed Yu-Shiba-Rusinov (or Andreev) quasiparticles.

TOPOGRAPHY AND SPATIAL EXTENT

Empirical data obtained from STM measurements for $NbSe_2$

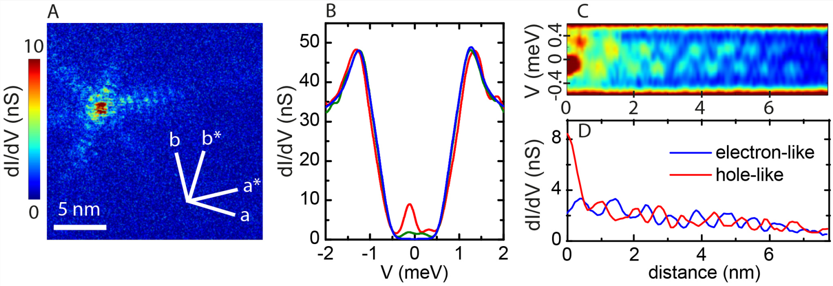

a) bound states extending to 10 nm (from impurity)

b) alternating particle and hole spectral weights

G.C. Menard et al., Nature Phys. 11, 1013 (2015).

MAGNETIC OBJECTS IN SUPERCONDUCTORS

Other entities in superconductors, like magnetic chains

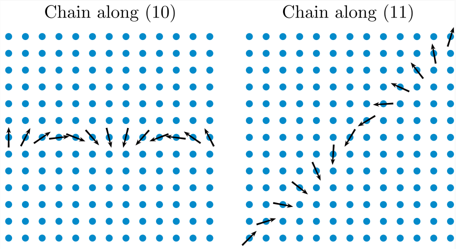

Other entities in superconductors, like magnetic chains

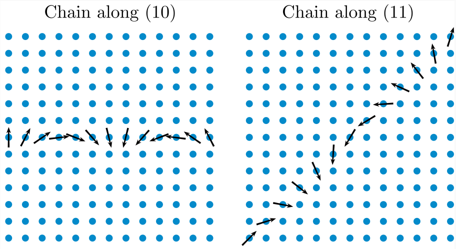

or magnetic islands

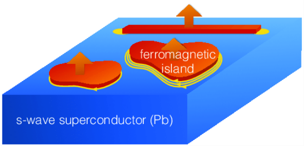

MAGNETIC OBJECTS IN SUPERCONDUCTORS

Other entities in superconductors, like magnetic chains

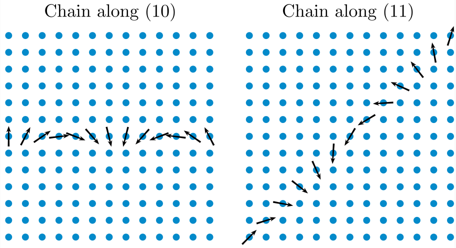

or magnetic islands

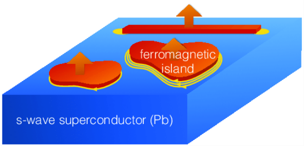

develop their in-gap bound states in a form of the Shiba-bands.

MAGNETIC OBJECTS IN SUPERCONDUCTORS

Other entities in superconductors, like magnetic chains

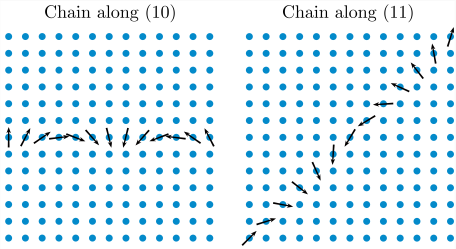

or magnetic islands

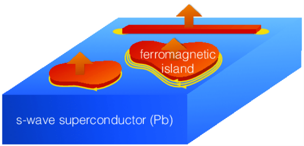

develop their in-gap bound states in a form of the <u>Shiba-bands.</u>

In particular, the proper magnetic textures in chains and islands can guarantee the topologically non-trivial character, hosting the Majorana-type boundary modes !

A few examples ...

1. Rashba nanowires

TOPOLOGICAL SUPERCONDUCTING NANOWIRE

Intersite pairing of identical spin electrons can be driven e.g. by spin-orbit (Rashba) interaction in presence of external magnetic field, using semiconducting nanowires proximitized to conventional *s-wave* superconductor.

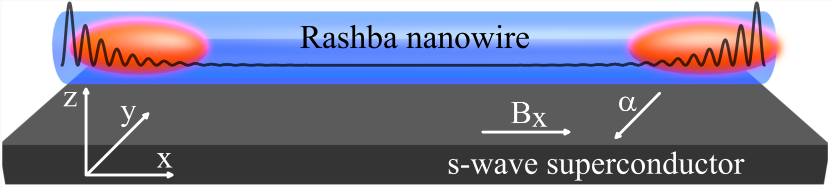

Effective quasiparticle states of the Rashba nanowire

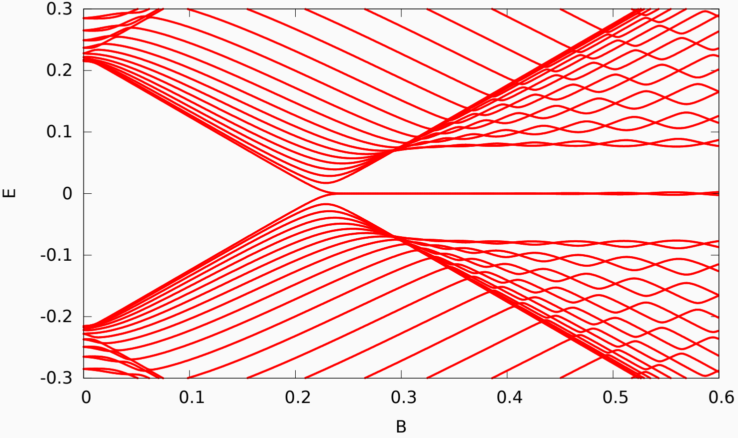

Effective quasiparticle states of the Rashba nanowire

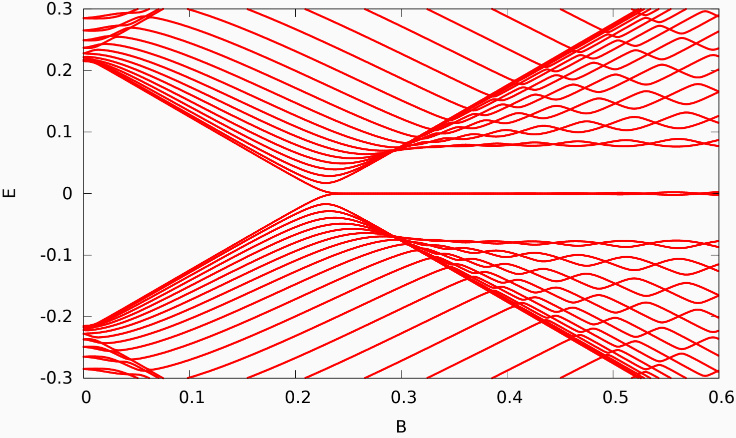

closing/reopening of a gap ⇔ band-invertion of topological insulators

M.M. Maśka, A. Gorczyca-Goraj, J. Tworzydło, T. Domański, PRB 95, 045429 (2017).

SPATIAL PROFILE OF MAJORANA QPS

Majorana qps are localized near the edges

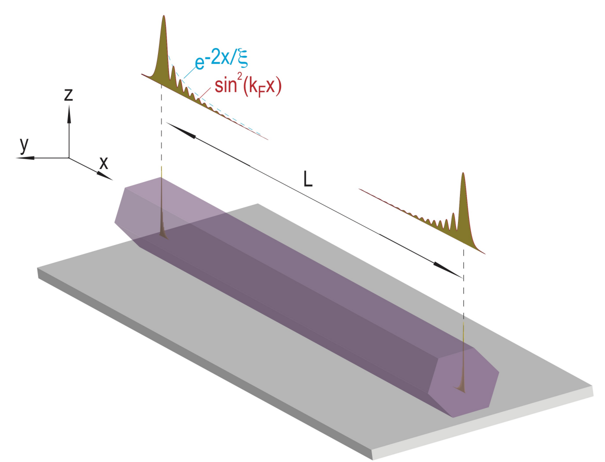

R. Aguado, Riv. Nuovo Cim. 40, 523 (2017).

Differential conductance dI/dV obtained for InSb nanowire at 70 mK upon varying a magnetic field.

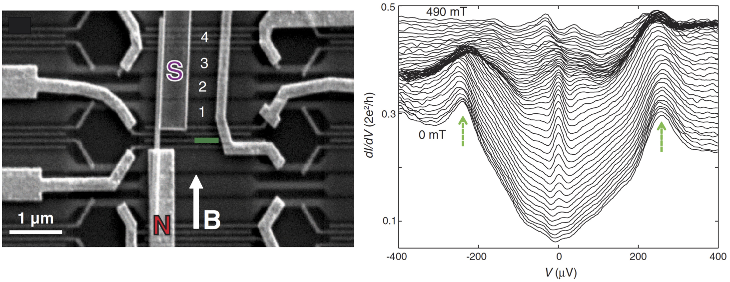

V. Mourik, ..., and L.P. Kouwenhoven, Science **336**, 1003 (2012).

/ Technical Univ. Delft, Netherlands /

EXAMPLE OF EMPIRICAL REALIZATION

Litographically fabricated Al nanowire contacted to InAs

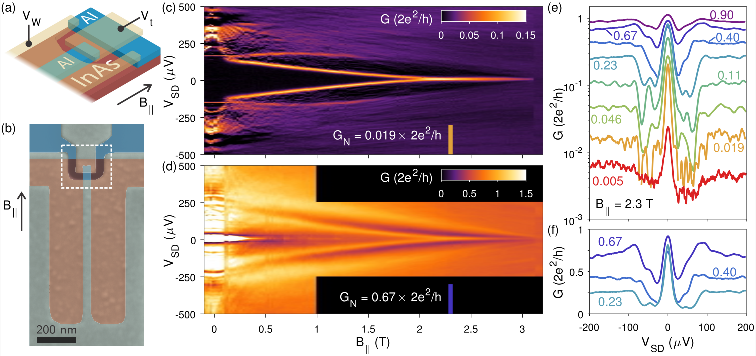

F. Nichele, ..., and Ch. Marcus, Phys. Rev. Lett. **119**, 136803 (2017).

/ Niels Bohr Institute, Copenhagen, Denmark /

2. Selforganised magnetic chains

MAGNETIC CHAINS ON SUPERCONDUCTORS

Magnetic atoms (like Fe) on a surface of s-wave superconductor (for example Pb) arrange themselves into such spiral order, where topological superconducting phase is selfsustained

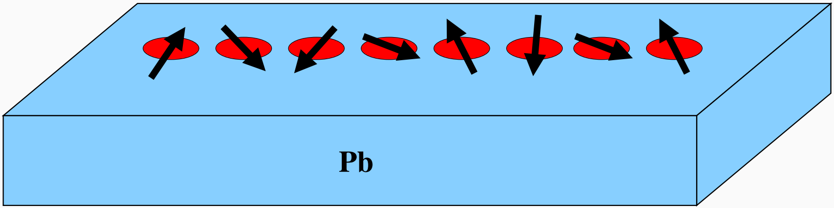

MICROSCOPIC MODEL

Itinerant electrons in the chain of magnetic impurities placed on a surface of isotropic superconductor can be described by the Hamiltonian:

MICROSCOPIC MODEL

Itinerant electrons in the chain of magnetic impurities placed on a surface of isotropic superconductor can be described by the Hamiltonian:

$$H = -\; t \sum_{i,\sigma} \left(\hat{c}^{\dagger}_{i,\sigma} \hat{c}_{i+1,\sigma} + \text{H.c.} \right) - \mu \sum_{i,\sigma} \hat{c}^{\dagger}_{i,\sigma} \hat{c}_{i,\sigma}$$

MICROSCOPIC MODEL

Itinerant electrons in the chain of magnetic impurities placed on a surface of isotropic superconductor can be described by the Hamiltonian:

$$
\begin{aligned}
H = & -t \sum_{i,\sigma} \left(\hat{c}^{\dagger}_{i,\sigma} \hat{c}_{i+1,\sigma} + \text{H.c.} \right) - \mu \sum_{i,\sigma} \hat{c}^{\dagger}_{i,\sigma} \hat{c}_{i,\sigma} \\
& + J \sum_{i} \vec{S}_i \cdot \hat{\vec{s}}_i + \sum_{i} \left(\Delta \hat{c}^{\dagger}_{i\uparrow} \hat{c}^{\dagger}_{i\downarrow} + \text{H.c.} \right)
\end{aligned}
$$

Itinerant electrons in the chain of magnetic impurities placed on a surface of isotropic superconductor can be described by the Hamiltonian:

$$H = - t \sum_{i,\sigma} \left(\hat{c}^{\dagger}_{i,\sigma} \hat{c}_{i+1,\sigma} + \mathrm{H.c.} \right) - \mu \sum_{i,\sigma} \hat{c}^{\dagger}_{i,\sigma} \hat{c}_{i,\sigma} + J \sum_{i} \vec{S}_i \cdot \hat{\vec{s}}_i + \sum_{i} \left(\Delta \hat{c}^{\dagger}_{i\uparrow} \hat{c}^{\dagger}_{i\downarrow} + \mathrm{H.c.} \right)$$

Here $\vec{S}_i$ are the classical magnetic moments and $\hat{\vec{s}}_i = \frac{1}{2} \sum_{\alpha,\beta} \hat{c}^{\dagger}_{i,\alpha} \vec{\sigma}_{\alpha\beta} \hat{c}_{i,\beta}$ denote the spins of mobile electrons

MICROSCOPIC MODEL

Itinerant electrons in the chain of magnetic impurities placed on a surface of isotropic superconductor can be described by the Hamiltonian:

$$\begin{aligned} H = & -t \sum_{i,\sigma} \left(\hat{c}^{\dagger}_{i,\sigma} \hat{c}_{i+1,\sigma} + \mathrm{H.c.} \right) - \mu \sum_{i,\sigma} \hat{c}^{\dagger}_{i,\sigma} \hat{c}_{i,\sigma} \\ & + J \sum_{i} \vec{S}_i \cdot \hat{\vec{s}}_i + \sum_{i} \left(\Delta \hat{c}^{\dagger}_{i\uparrow} \hat{c}^{\dagger}_{i\downarrow} + \mathrm{H.c.} \right) \end{aligned}$$

Here $\vec{S}_i$ are the classical magnetic moments and $\hat{\vec{s}}_i = \frac{1}{2} \sum_{\alpha,\beta} \hat{c}^{\dagger}_{i,\alpha} \vec{\sigma}_{\alpha\beta} \hat{c}_{i,\beta}$ denote the spins of mobile electrons

$\Longrightarrow$ **J is the coupling between magnetic atoms and itinerant electrons**

MICROSCOPIC MODEL

Itinerant electrons in the chain of magnetic impurities placed on a surface of isotropic superconductor can be described by the Hamiltonian:

$$H = -\ t \sum_{i,\sigma} \left(\hat{c}^\dagger_{i,\sigma} \hat{c}_{i+1,\sigma} + \text{H.c.} \right) - \mu \sum_{i,\sigma} \hat{c}^\dagger_{i,\sigma} \hat{c}_{i,\sigma}$$
$$+\ J \sum_{i} \vec{S}_i \cdot \hat{\vec{s}}_i + \sum_i \left(\Delta \hat{c}^\dagger_{i\uparrow} \hat{c}^\dagger_{i\downarrow} + \text{H.c.} \right)$$

Here $\vec{S}_i$ are the classical magnetic moments and $\hat{\vec{s}}_i = \frac{1}{2} \sum_{\alpha,\beta} \hat{c}^\dagger_{i,\alpha} \vec{\sigma}_{\alpha\beta} \hat{c}_{i,\beta}$ denote the spins of mobile electrons

$\Longrightarrow$ J **is the coupling between magnetic atoms and itinerant electrons**

$\Longrightarrow$ Δ **is the proximity induced on-site pairing**

OUTLINE OF COMPUTATIONAL PROCEDURE

We have focused on coplanar arrangement of the magnetic moments

$$\vec{S}_i = S\left(\cos\phi_i,\ \sin\phi_i,\ 0\right)$$

OUTLINE OF COMPUTATIONAL PROCEDURE

We have focused on coplanar arrangement of the magnetic moments

$$\vec{S}_i = S\,(\cos\phi_i,\ \sin\phi_i,\ 0)$$

assuming S to be large, while the product JS was imposed to be finite (classical treatment of magnetic moments).

OUTLINE OF COMPUTATIONAL PROCEDURE

We have focused on coplanar arrangement of the magnetic moments

$$\vec{S}_i = S\,(\cos\phi_i,\ \sin\phi_i,\ 0)$$

assuming S to be large, while the product JS was imposed to be finite (classical treatment of magnetic moments).

We selfconsistently determined the spiral texture of a ground state:

OUTLINE OF COMPUTATIONAL PROCEDURE

We have focused on coplanar arrangement of the magnetic moments

$$\vec{S}_i = S\,(\cos\phi_i,\ \sin\phi_i,\ 0)$$

assuming S to be large, while the product JS was imposed to be finite (classical treatment of magnetic moments).

We selfconsistently determined the spiral texture of a ground state:

$$\Longrightarrow \quad \phi_i = i\; a\; q$$

OUTLINE OF COMPUTATIONAL PROCEDURE

We have focused on coplanar arrangement of the magnetic moments

$$\vec{S}_i = S\,(\cos\phi_i,\ \sin\phi_i,\ 0)$$

assuming S to be large, while the product JS was imposed to be finite (classical treatment of magnetic moments).

We selfconsistently determined the spiral texture of a ground state:

$$\Longrightarrow \quad \phi_i = i\ a\ q$$

where a is the lattice constant and the spiral pitch q strongly depends on the model parameters μ, Δ.

HELICAL SELFORGANISATION (TOPOFILIA)

A. Gorczyca-Goraj, T. Domański & M.M. Maśka, Phys. Rev. B 99, 235430 (2019).

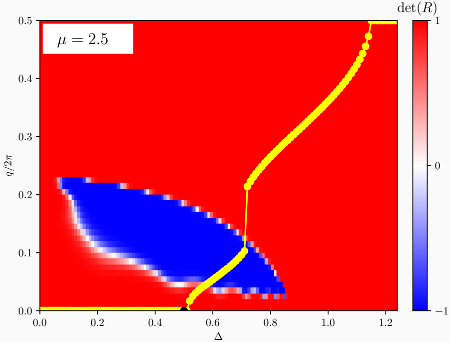

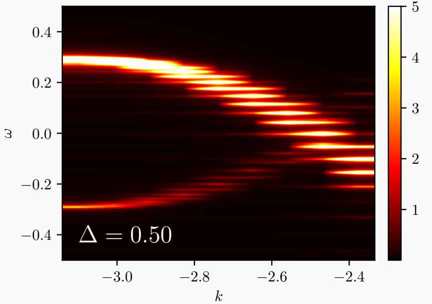

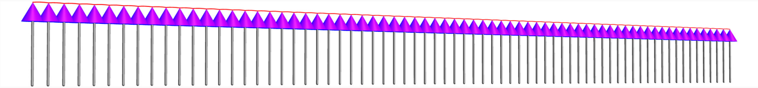

HELICAL SELFORGANISATION (TOPOFILIA)

A. Gorczyca-Goraj, T. Domański & M.M. Maśka, Phys. Rev. B 99, 235430 (2019).

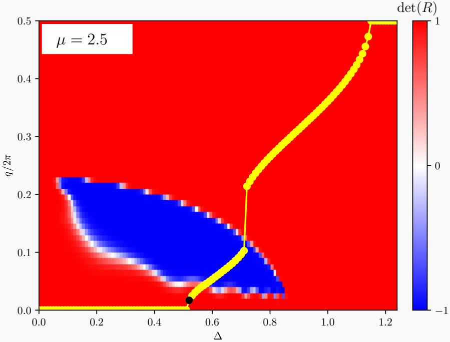

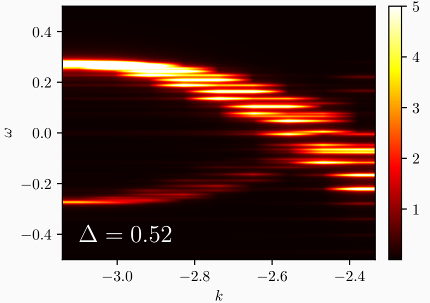

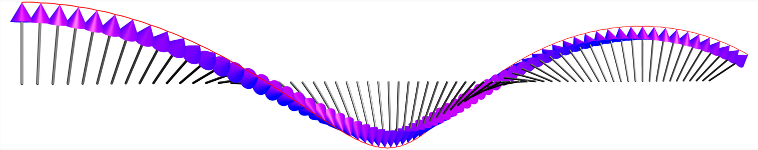

HELICAL SELFORGANISATION (TOPOFILIA)

A. Gorczyca-Goraj, T. Domański & M.M. Maśka, Phys. Rev. B 99, 235430 (2019).

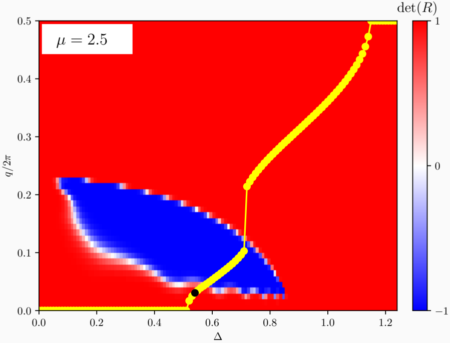

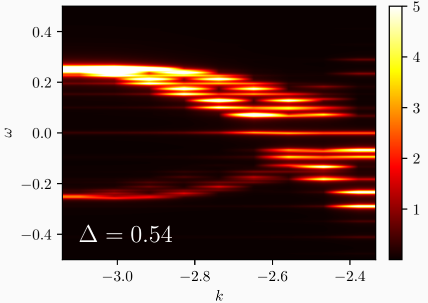

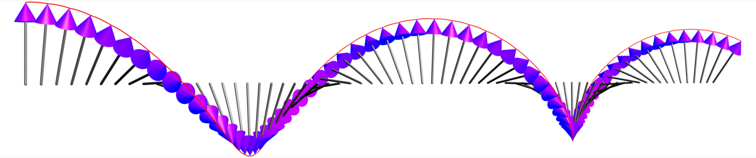

HELICAL SELFORGANISATION (TOPOFILIA)

A. Gorczyca-Goraj, T. Domański & M.M. Maśka, Phys. Rev. B <u>99</u>, 235430 (2019).

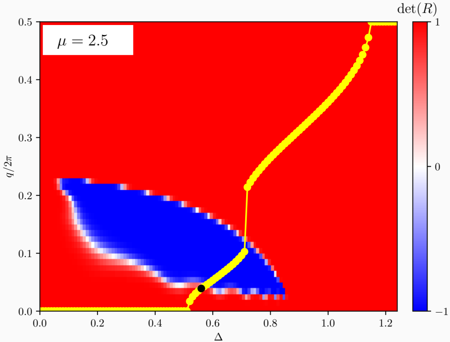

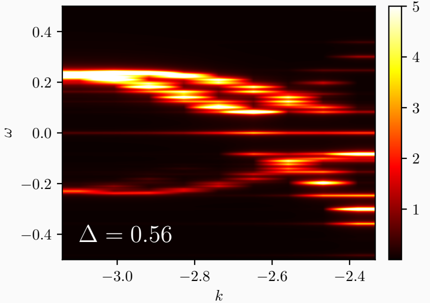

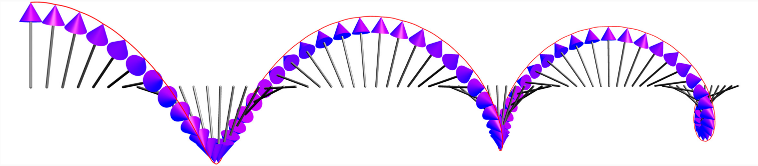

HELICAL SELFORGANISATION (TOPOFILIA)

A. Gorczyca-Goraj, T. Domański & M.M. Maśka, Phys. Rev. B 99, 235430 (2019).

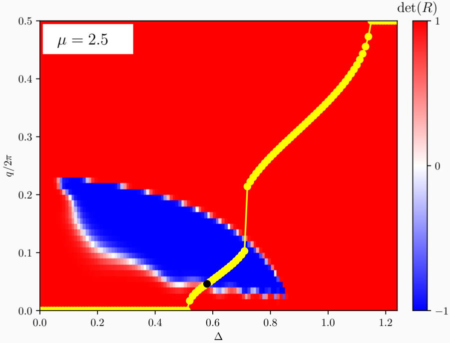

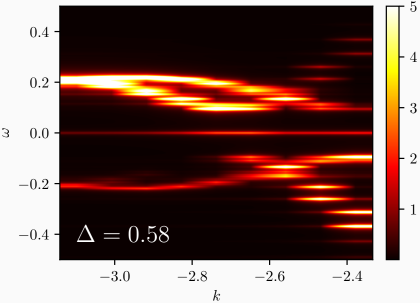

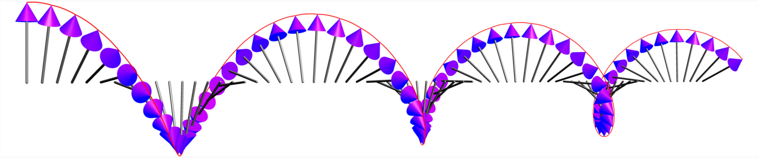

HELICAL SELFORGANISATION (TOPOFILIA)

A. Gorczyca-Goraj, T. Domański & M.M. Maśka, Phys. Rev. B 99, 235430 (2019).

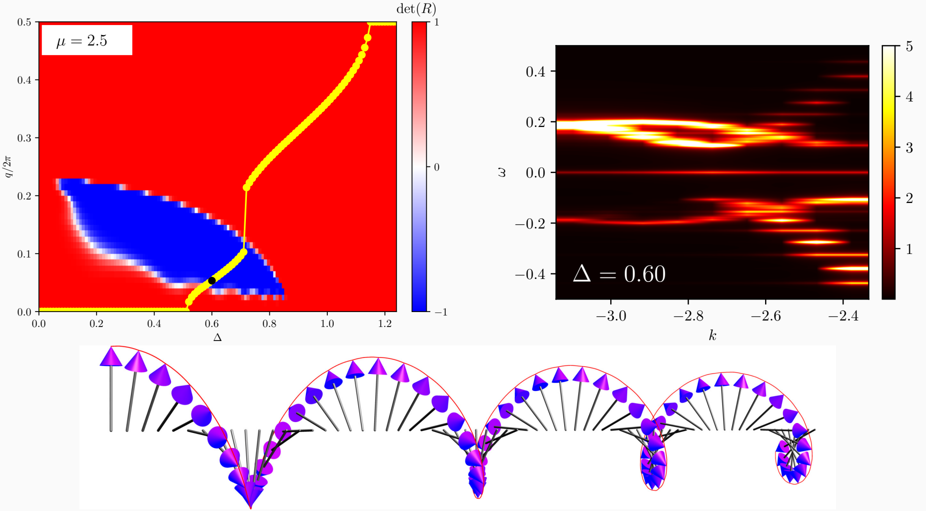

HELICAL SELFORGANISATION (TOPOFILIA)

A. Gorczyca-Goraj, T. Domański & M.M. Maśka, Phys. Rev. B 99, 235430 (2019).

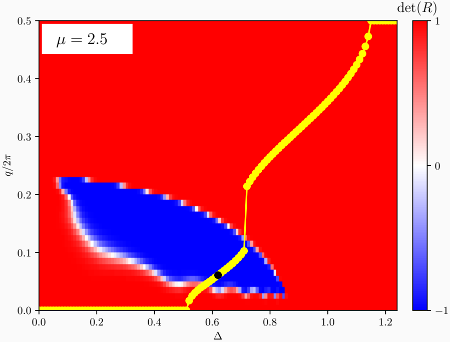

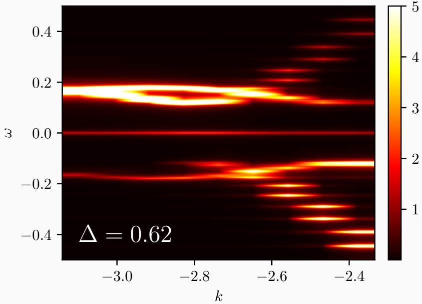

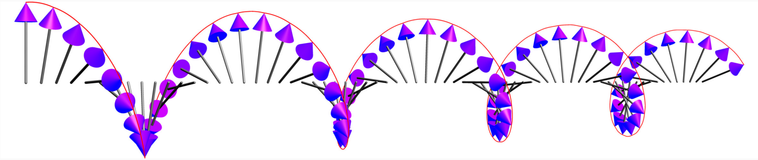

HELICAL SELFORGANISATION (TOPOFILIA)

A. Gorczyca-Goraj, T. Domański & M.M. Maśka, Phys. Rev. B 99, 235430 (2019).

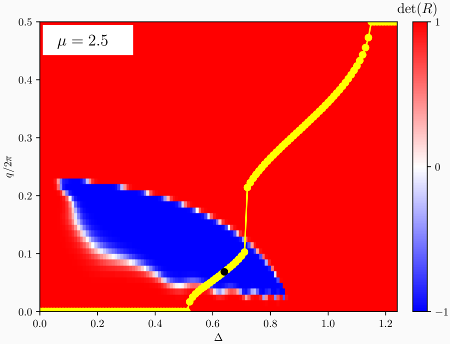

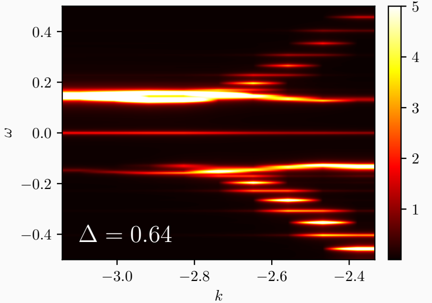

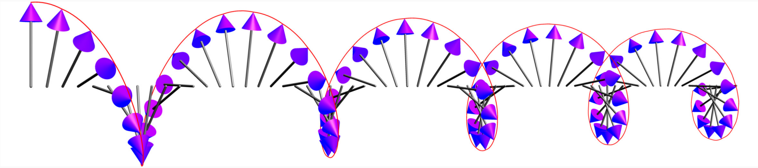

HELICAL SELFORGANISATION (TOPOFILIA)

A. Gorczyca-Goraj, T. Domański & M.M. Maśka, Phys. Rev. B 99, 235430 (2019).

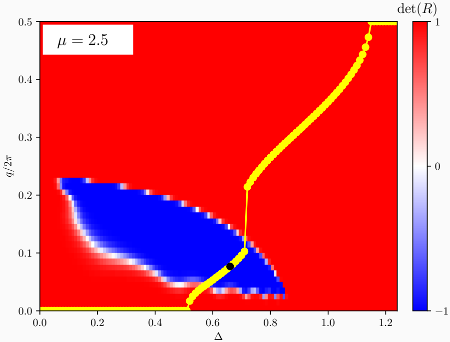

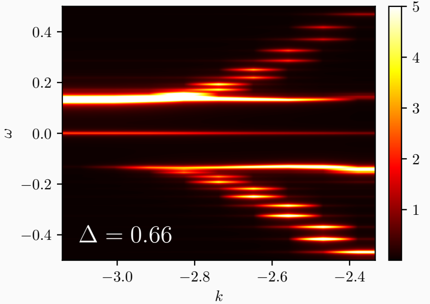

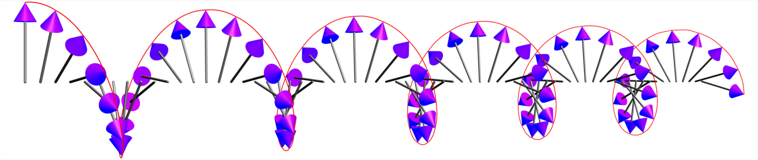

HELICAL SELFORGANISATION (TOPOFILIA)

A. Gorczyca-Goraj, T. Domański & M.M. Maśka, Phys. Rev. B 99, 235430 (2019).

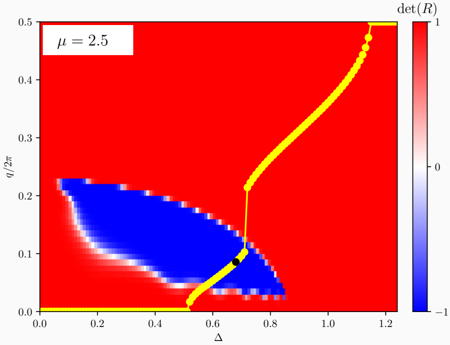

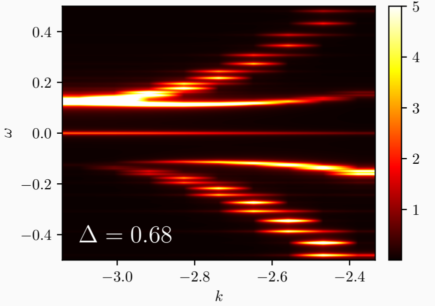

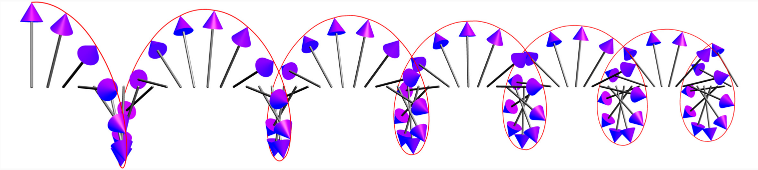

HELICAL SELFORGANISATION (TOPOFILIA)

A. Gorczyca-Goraj, T. Domański & M.M. Maśka, Phys. Rev. B 99, 235430 (2019).

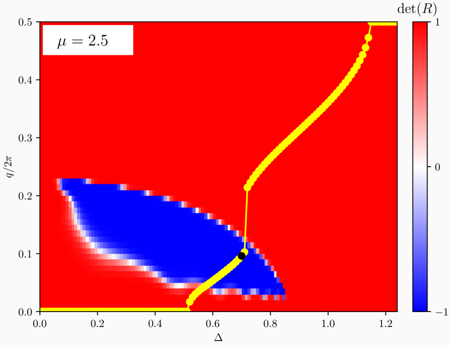

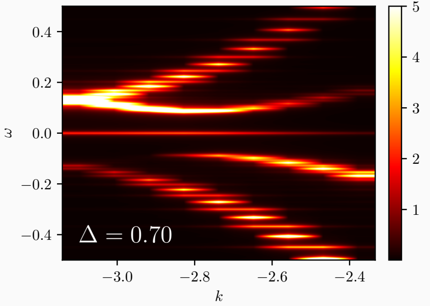

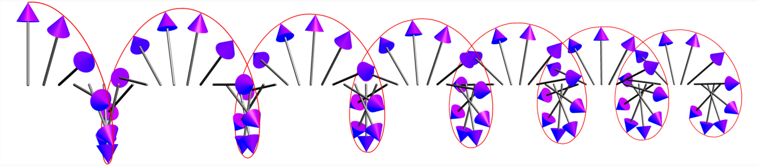

HELICAL SELFORGANISATION (TOPOFILIA)

A. Gorczyca-Goraj, T. Domański & M.M. Maśka, Phys. Rev. B 99, 235430 (2019).

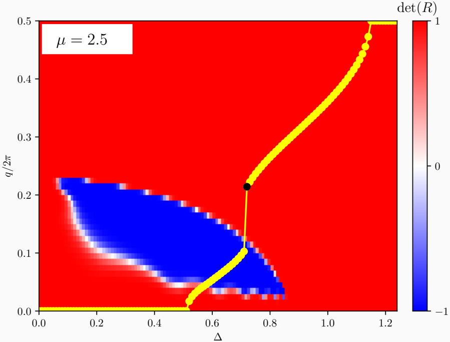

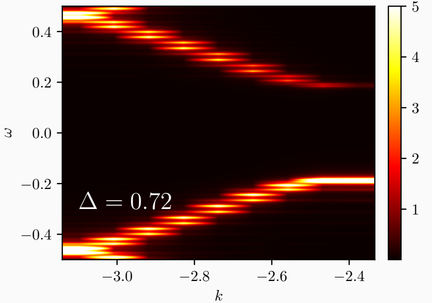

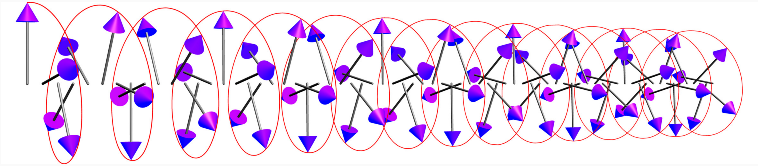

SPIRAL ORDER AT FINITE TEMPERATURES

Structure factor: $A(q) = \frac{1}{L} \sum_{jk} e^{iq(j-k)} \langle \vec{S}_j \cdot \vec{S}_k \rangle$

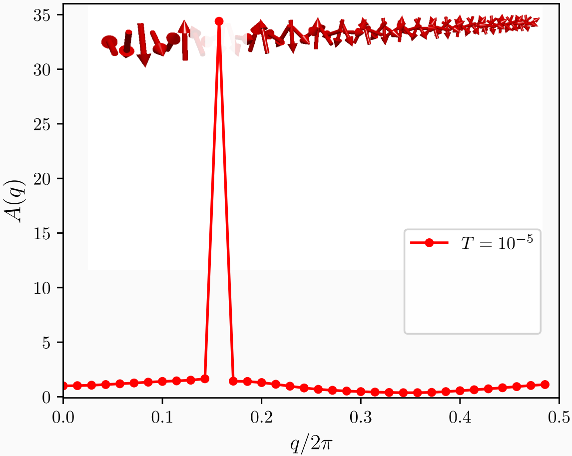

SPIRAL ORDER AT FINITE TEMPERATURES

Structure factor: $A(q) = \frac{1}{L} \sum_{jk} e^{iq(j-k)} \langle \vec{S}_j \cdot \vec{S}_k \rangle$

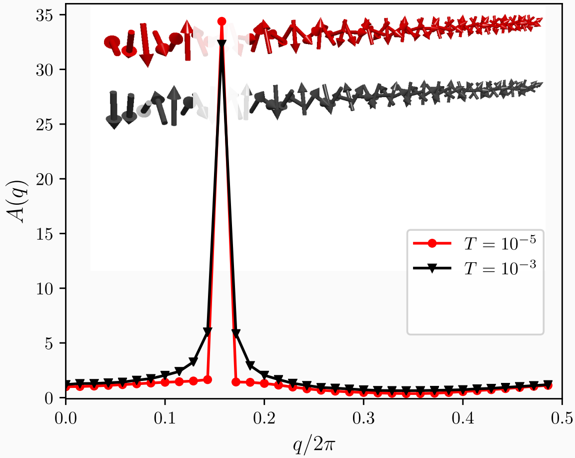

SPIRAL ORDER AT FINITE TEMPERATURES

Structure factor: $A(q) = \frac{1}{L} \sum_{jk} e^{iq(j-k)} \langle \vec{S}_j \cdot \vec{S}_k \rangle$

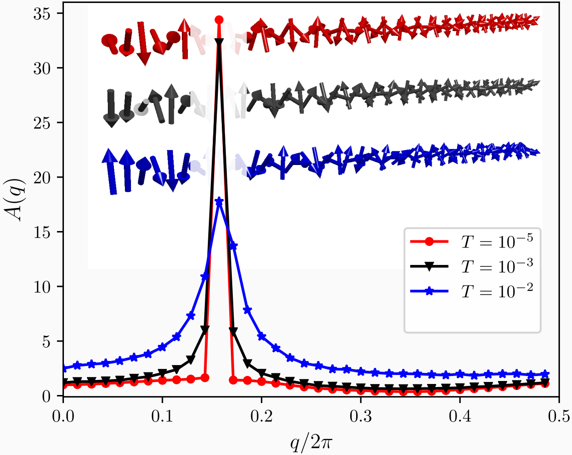

SPIRAL ORDER AT FINITE TEMPERATURES

Structure factor: $A(q) = \frac{1}{L} \sum_{jk} e^{iq(j-k)} \langle \vec{S}_j \cdot \vec{S}_k \rangle$

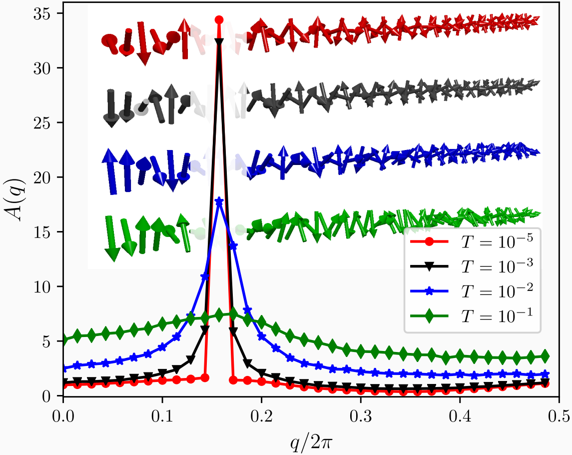

TEMPERATURE EFFECT ON MAJORANA QPS

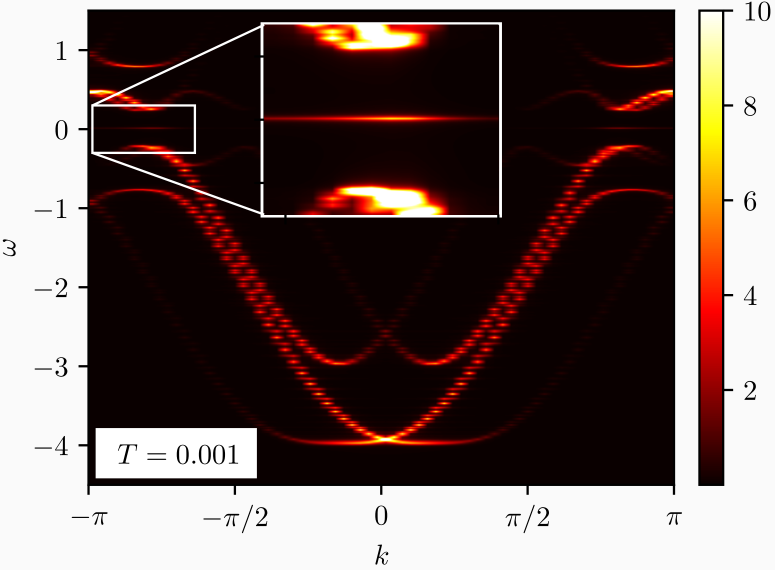

INFLUENCE OF TEMPERATURE ON MAJORANA QPS

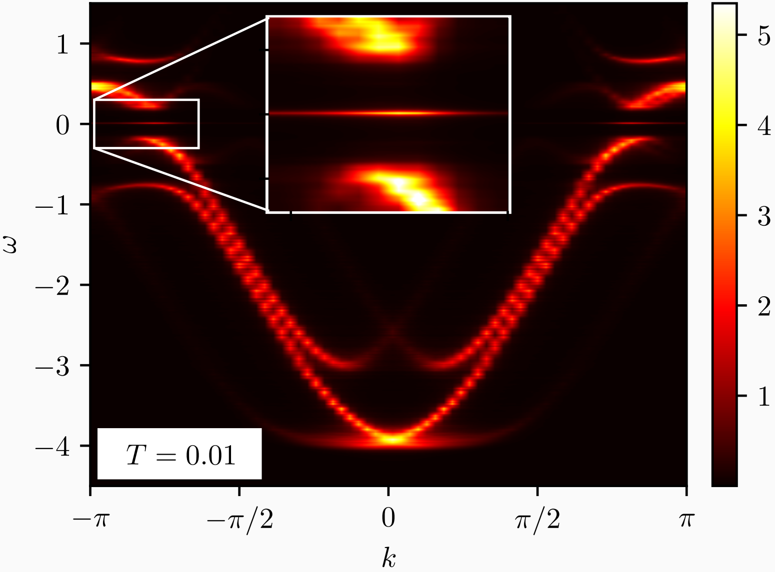

INFLUENCE OF TEMPERATURE ON MAJORANA QPS

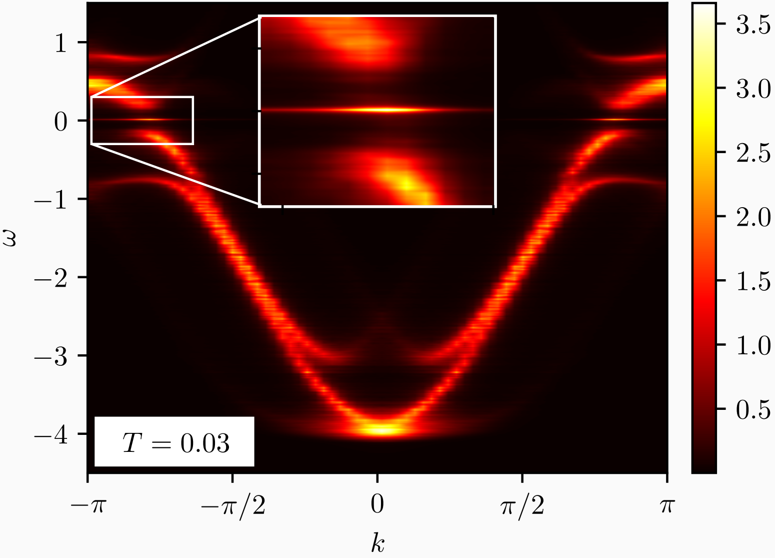

INFLUENCE OF TEMPERATURE ON MAJORANA QPS

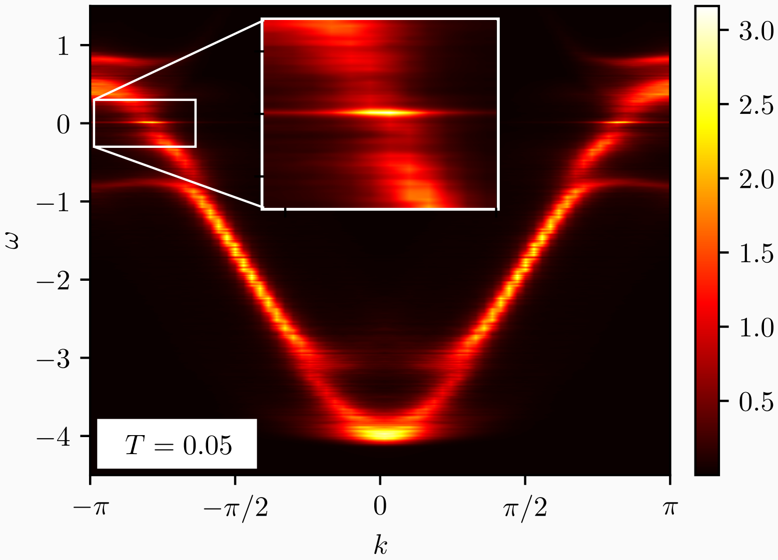

INFLUENCE OF TEMPERATURE ON MAJORANA QPS

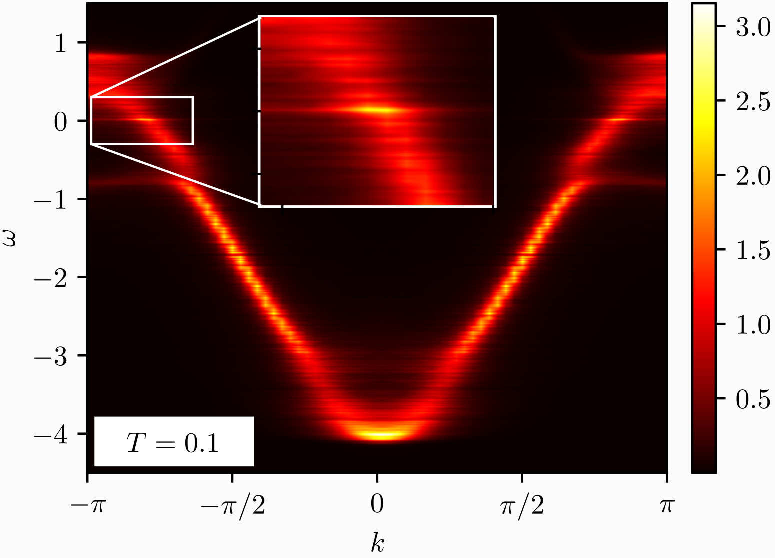

INFLUENCE OF TEMPERATURE ON MAJORANA QPS

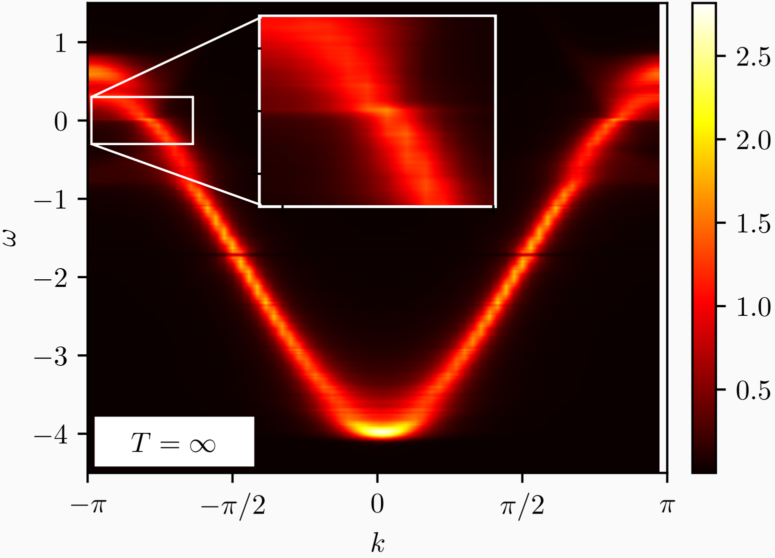

ROLE OF THERMAL EFFECTS

Upon increasing the temperature one observes:

$\Longrightarrow$ **closing of the topological energy gap**

$\Longrightarrow$ **overdamping of the Majorana qps**

$\Longrightarrow$ **changeover of topological $\mathbb{Z}_2$ number**

ROLE OF THERMAL EFFECTS

Upon increasing the temperature one observes:

$\Longrightarrow$ **closing of the topological energy gap**

$\Longrightarrow$ **overdamping of the Majorana qps**

$\Longrightarrow$ **changeover of topological $\mathbb{Z}_2$ number**

In realistic situations (using, for instance, Fe atoms deposited on superconducting Pb) the topological phase should survive up to:

$\Longrightarrow$ $T_c \approx$ **5 K**

3. Selforganised magnetic ladders

TOPOLOGICAL MAGNETIC LADDER

Let's consider magnetic ladder deposited on conventinal superconductor.

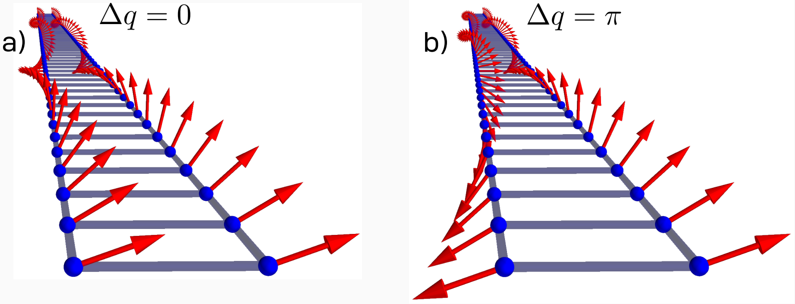

M.M. Maśka, N. Sedlmayr, A. Kobiałka, T. Domański, Phys. Rev. B 103, 235419 (2021).

MICROSCOPIC MODEL

Itinerant electrons on the magnetic ladder which is proximitized to superconducting substrate can be described by the Hamiltonian:

MICROSCOPIC MODEL

Itinerant electrons on the magnetic ladder which is proximitized to superconducting substrate can be described by the Hamiltonian:

$$H = -t\sum_{i,\sigma}\left(\sum_{j}\hat{c}^{\dagger}_{i,j,\sigma}\hat{c}_{i+1,j,\sigma} + \hat{c}^{\dagger}_{i,1,\sigma}\hat{c}_{i,2,\sigma} + \mathbf{H.c.}\right) - \mu\sum_{i,j,\sigma}\hat{c}^{\dagger}_{i,j,\sigma}\hat{c}_{i,j,\sigma}$$

MICROSCOPIC MODEL

Itinerant electrons on the magnetic ladder which is proximitized to superconducting substrate can be described by the Hamiltonian:

$$\begin{aligned} H &= -t\sum_{i,\sigma}\left(\sum_{j}\hat{c}^{\dagger}_{i,j,\sigma}\hat{c}_{i+1,j,\sigma}+\hat{c}^{\dagger}_{i,1,\sigma}\hat{c}_{i,2,\sigma}+\mathrm{H.c.}\right)-\mu\sum_{i,j,\sigma}\hat{c}^{\dagger}_{i,j,\sigma}\hat{c}_{i,j,\sigma} \\ &\quad +J\sum_{i,j}\vec{S}_{i,j}\cdot\hat{\vec{s}}_{i,j} \end{aligned}$$

MICROSCOPIC MODEL

Itinerant electrons on the magnetic ladder which is proximitized to superconducting substrate can be described by the Hamiltonian:

$$
\begin{aligned}
H \;=\; & -t\sum_{i,\sigma}\left(\sum_{j}\hat{c}^{\dagger}_{i,j,\sigma}\hat{c}_{i+1,j,\sigma}+\hat{c}^{\dagger}_{i,1,\sigma}\hat{c}_{i,2,\sigma}+\mathrm{H.c.}\right)-\mu\sum_{i,j,\sigma}\hat{c}^{\dagger}_{i,j,\sigma}\hat{c}_{i,j,\sigma} \\
& +J\sum_{i,j}\vec{S}_{i,j}\cdot\hat{\vec{s}}_{i,j}+\Delta\sum_{i,j}\left(\hat{c}^{\dagger}_{i,j,\uparrow}\;\hat{c}^{\dagger}_{i,j,\downarrow}+\mathrm{H.c.}\right)
\end{aligned}
$$

MICROSCOPIC MODEL

Itinerant electrons on the magnetic ladder which is proximitized to superconducting substrate can be described by the Hamiltonian:

$$\begin{aligned} H \;=\;& -t\sum_{i,\sigma}\left(\sum_{j}\hat{c}^{\dagger}_{i,j,\sigma}\hat{c}_{i+1,j,\sigma}+\hat{c}^{\dagger}_{i,1,\sigma}\hat{c}_{i,2,\sigma}+\mathrm{H.c.}\right)-\mu\sum_{i,j,\sigma}\hat{c}^{\dagger}_{i,j,\sigma}\hat{c}_{i,j,\sigma} \\ & +J\sum_{i,j}\vec{S}_{i,j}\cdot\hat{\vec{s}}_{i,j}+\Delta\sum_{i,j}\left(\hat{c}^{\dagger}_{i,j,\uparrow}\;\hat{c}^{\dagger}_{i,j,\downarrow}+\mathrm{H.c.}\right) \end{aligned}$$

where $\vec{S}_{i,j}$ are classical magnetic moments, and

MICROSCOPIC MODEL

Itinerant electrons on the magnetic ladder which is proximitized to superconducting substrate can be described by the Hamiltonian:

$$
\begin{aligned}
H \quad = \quad & -t\sum_{i,\sigma}\left(\sum_{j}\hat{c}^{\dagger}_{i,j,\sigma}\hat{c}_{i+1,j,\sigma}+\hat{c}^{\dagger}_{i,1,\sigma}\hat{c}_{i,2,\sigma}+\mathbf{H.c.}\right)-\mu\sum_{i,j,\sigma}\hat{c}^{\dagger}_{i,j,\sigma}\hat{c}_{i,j,\sigma} \\
& +J\sum_{i,j}\vec{S}_{i,j}\cdot\hat{\vec{s}}_{i,j}+\Delta\sum_{i,j}\left(\hat{c}^{\dagger}_{i,j,\uparrow}\ \hat{c}^{\dagger}_{i,j,\downarrow}+\mathbf{H.c.}\right)
\end{aligned}
$$

where $\vec{S}_{i,j}$ are classical magnetic moments, and

$\Longrightarrow$ **where $i=1,2,\ldots N$ enumerates sites along the wires**

MICROSCOPIC MODEL

Itinerant electrons on the magnetic ladder which is proximitized to superconducting substrate can be described by the Hamiltonian:

$$\begin{aligned} H \;=\;& -t \sum_{i,\sigma} \left(\sum_j \hat{c}^\dagger_{i,j,\sigma} \hat{c}_{i+1,j,\sigma} + \hat{c}^\dagger_{i,1,\sigma} \hat{c}_{i,2,\sigma} + \mathrm{H.c.} \right) - \mu \sum_{i,j,\sigma} \hat{c}^\dagger_{i,j,\sigma} \hat{c}_{i,j,\sigma} \\ & + J \sum_{i,j} \vec{S}_{i,j} \cdot \hat{\vec{s}}_{i,j} + \Delta \sum_{i,j} \left(\hat{c}^\dagger_{i,j,\uparrow} \; \hat{c}^\dagger_{i,j,\downarrow} + \mathrm{H.c.} \right) \end{aligned}$$

where $\vec{S}_{i,j}$ are classical magnetic moments, and

$\Longrightarrow$ **where $i = 1, 2, \ldots N$ enumerates sites along the wires**

$\Longrightarrow$ **$j \in \{1, 2\}$ refers to the legs**

OUTLINE OF COMPUTATIONAL PROCEDURE

We have investigated a coplanar arrangement of the magnetic moments

$$\vec{S}_{i,j} = S\left(\cos\phi_{i,j},\ \sin\phi_{i,j},\ 0\right)$$

OUTLINE OF COMPUTATIONAL PROCEDURE

We have investigated a coplanar arrangement of the magnetic moments

$$\vec{S}_{i,j} = S\left(\cos\phi_{i,j},\ \sin\phi_{i,j},\ 0\right)$$

assuming S to be large, and imposing the product JS to be finite.

OUTLINE OF COMPUTATIONAL PROCEDURE

We have investigated a coplanar arrangement of the magnetic moments

$$\vec{S}_{i,j} = S\left(\cos\phi_{i,j},\ \sin\phi_{i,j},\ 0\right)$$

assuming S to be large, and imposing the product JS to be finite.

We have selfconsistently determined the helical configuration of a ground state, characterized by:

OUTLINE OF COMPUTATIONAL PROCEDURE

We have investigated a coplanar arrangement of the magnetic moments

$$\vec{S}_{i,j} = S\left(\cos\phi_{i,j},\ \sin\phi_{i,j},\ 0\right)$$

assuming S to be large, and imposing the product JS to be finite.

We have selfconsistently determined the helical configuration of a ground state, characterized by:

$\Longrightarrow$ $\phi_{i,1} = i\ q$ (q is the spiral pitch)

OUTLINE OF COMPUTATIONAL PROCEDURE

We have investigated a coplanar arrangement of the magnetic moments

$$\vec{S}_{i,j} = S\left(\cos\phi_{i,j},\ \sin\phi_{i,j},\ 0\right)$$

assuming S to be large, and imposing the product JS to be finite.

We have selfconsistently determined the helical configuration of a ground state, characterized by:

$\Longrightarrow$ $\phi_{i,1} = i\ q$ **(q is the spiral pitch)**

$\Longrightarrow$ $\phi_{i,2} = i\ q + \Delta q$ **(Δq is phase difference between the legs)**

MAGNETIC SELFORGANIZATION

The ground state pitch vector $q_\star$ and relative phase $\Delta q_\star$ obtained with respect of the chemical potential μ and pairing potential Δ.

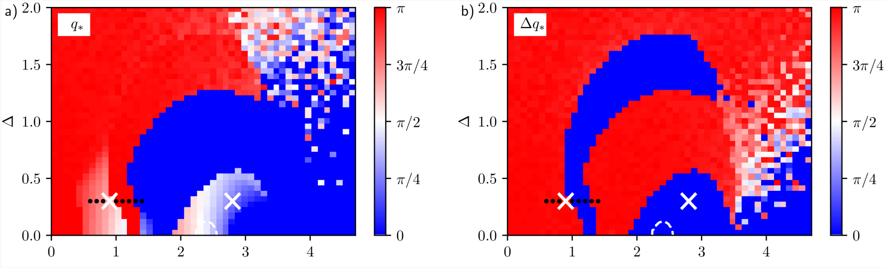

μ [in units of t] **μ**

Most parts of the diagrams correspond either to ferromagnetic or antiferromagnetic order,

MAGNETIC SELFORGANIZATION

The ground state pitch vector $q_\star$ and relative phase $\Delta q_\star$ obtained with respect of the chemical potential μ and pairing potential Δ.

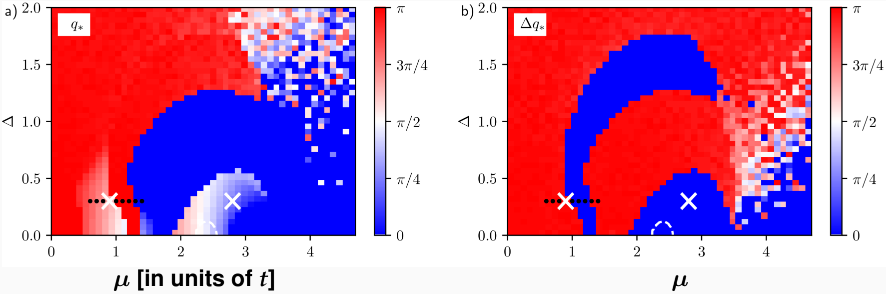

Most parts of the diagrams correspond either to ferromagnetic or antiferromagnetic order, except small regions where the helical order is developed (of our interest).

TOPOLOGICAL INVARIANT

In the thermodynamic limit ($N \to \infty$) we have determine the topological $\mathbb{Z}$ invariant of this system, which belongs to class AIII.

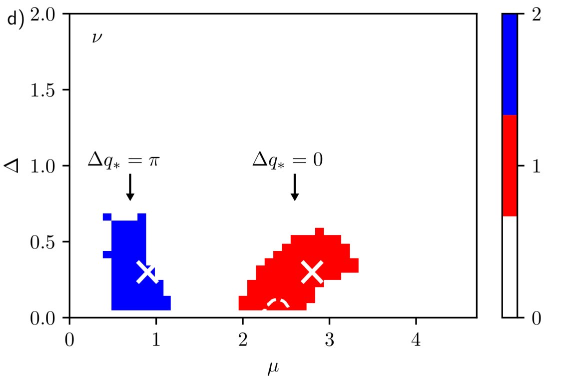

Two (separate) regions of the topological superconducting phase are characterized by either antiparallel or parallel spiral arrangements of the magnetic ladder.

For both these regions of $(\boldsymbol{\Delta}, \boldsymbol{\mu})$ the system is in a topologically nontrivial superconducting state, hosting the zero-energy boundary modes.

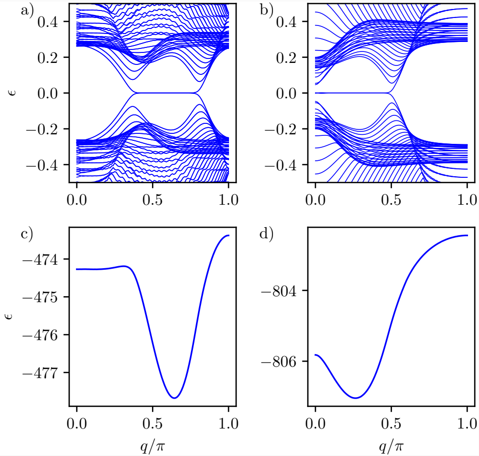

Eigenenergies (top) and total energy (bottom) for $\mu = 0.9$ (left) and $\mu = 2.8$ (right).

TRANSITION TO/FROM TOPOLOGICAL PHASE

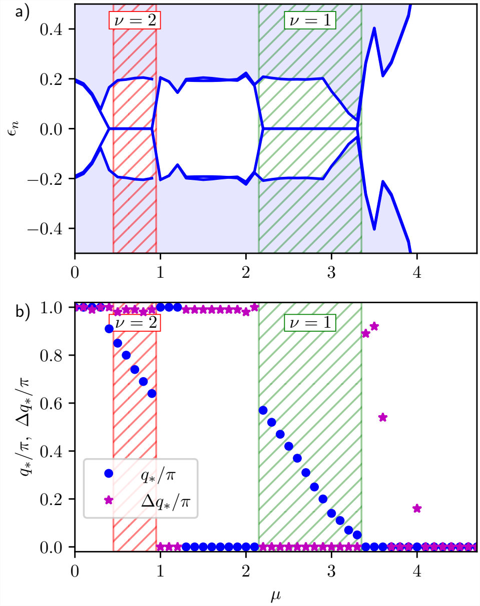

Variation of eigenenergies ε_n against μ for $\Delta = 0.3$

Variation of $q_\star$ and $\Delta q_\star$

TRANSITION TO/FROM TOPOLOGICAL PHASE

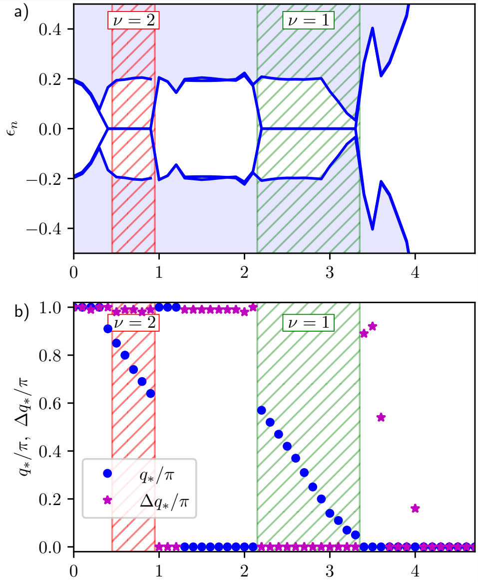

Variation of eigenenergies ε_n against μ for $\Delta = 0.3$

Variation of $q_\star$ and $\Delta q_\star$

Discontinuous transitions to/from topological phase without gap closing!

DISCONTINUOUS TRANSITIONS

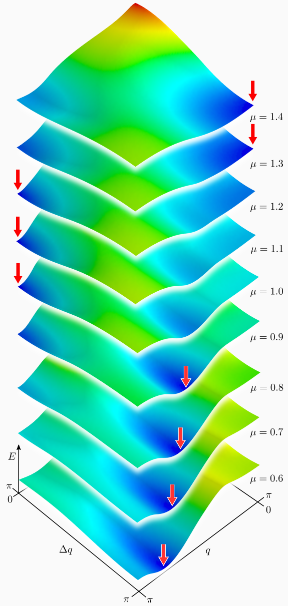

Total energy as function of q and Δq obtained for $\Delta = 0.3t$ and several μ.

DISCONTINUOUS TRANSITIONS

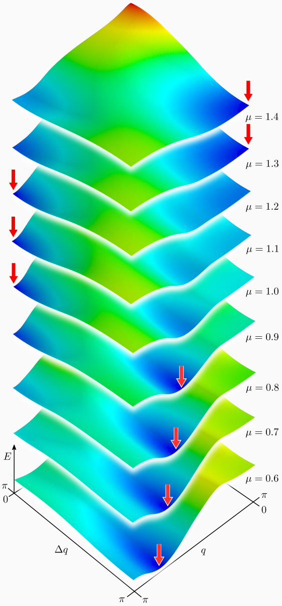

Total energy as function of q and Δq obtained for $\Delta = 0.3t$ and several μ.

The red arrow indicates $(q_\star, \Delta q_\star)$.

MAIN FINDINGS

We predict unconventional transition to/from topological superconducting phase of selforganized magnetic ladder

$\Rightarrow$ **without any closing/reopening of energy gap**

MAIN FINDINGS

We predict unconventional transition to/from topological superconducting phase of selforganized magnetic ladder

$\Rightarrow$ without any closing/reopening of energy gap

Upon varying the chemical potential (by electrostatic means) the emerging topological phase is characterized by:

$\Rightarrow$ either parallel or antiparallel helical structures

MAIN FINDINGS

We predict unconventional transition to/from topological superconducting phase of selforganized magnetic ladder

$\Longrightarrow$ **without any closing/reopening of energy gap**

Upon varying the chemical potential (by electrostatic means) the emerging topological phase is characterized by:

$\Longrightarrow$ **either parallel or antiparallel helical structures**

These topological phases differ by the value of:

$\Longrightarrow$ **topologoical invariant $\mathbb{Z}$**

MAIN FINDINGS

We predict unconventional transition to/from topological superconducting phase of selforganized magnetic ladder

$\Rightarrow$ **without any closing/reopening of energy gap**

Upon varying the chemical potential (by electrostatic means) the emerging topological phase is characterized by:

$\Rightarrow$ **either parallel or antiparallel helical structures**

These topological phases differ by the value of:

$\Rightarrow$ **topologoical invariant** $\mathbb{Z}$

M.M. Maśka, N. Sedlmayr, A. Kobiałka, T. Domański, Phys. Rev. B 103, 235419 (2021).

BEYOND COPLANAR CONFIGURATIONS

a) $\mu = 0.2$

b) $\mu = 0.6$

c) $\mu = 1.6$

d) $\mu = 3.2$

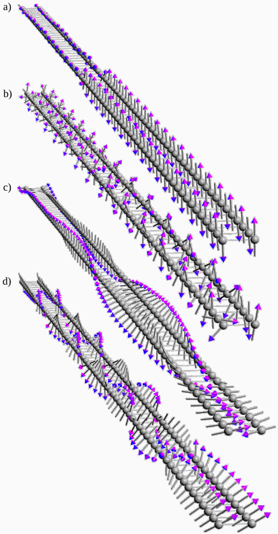

Unconstrained spin configurations obtained by the simulated annealing algorithm, performing the Metropolis Monte Carlo calculations (at low temperatures).

BOUNDARY ZERO-ENERGY MODES

The local Majorana polarization $\mathcal{P}_{i,j\sigma} = \langle\psi_\sigma|\mathcal{C}\hat{r}_{i,j}|\psi_\sigma\rangle$, where $\hat{r}_{i,j}$ is the projection onto site i of j-th chain and $\mathcal{C}$ stands for the particle-hole operator. Results are obtained for $\mu = 3.2$.

BOUNDARY ZERO-ENERGY MODES

The local Majorana polarization $\mathcal{P}_{i,j\sigma} = \langle \psi_\sigma | \mathcal{C} \hat{r}_{i,j} | \psi_\sigma \rangle$, where $\hat{r}_{i,j}$ is the projection onto site i of j-th chain and $\mathcal{C}$ stands for the particle-hole operator. Results are obtained for $\mu = 3.2$.

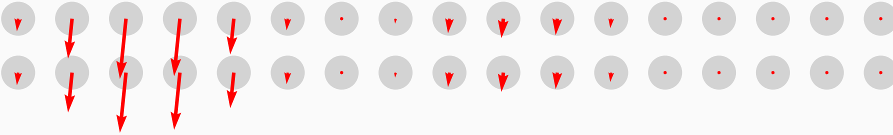

The topological superconducting phase & its boundary zero-energy modes are robust against a lack of coplanar helicity.

Higher-dimensional topological textures

TWO-DIMENSIONAL MAGNETIC STRUCTURES

Magnetic island of Co atoms deposited on the superconducting Pb surface

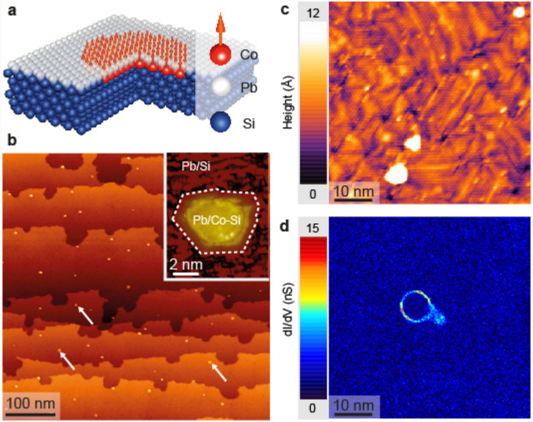

Diameter of island:

5 – 10 nm

G. Ménard, ..., and P. Simon, Nature Commun. 8, 2040 (2017).

Pierre & Marie Curie University (Paris, France)

PROPAGATING MAJORANA EDGE MODES

Magnetic island of Fe atoms deposited on the superconducting Re surface

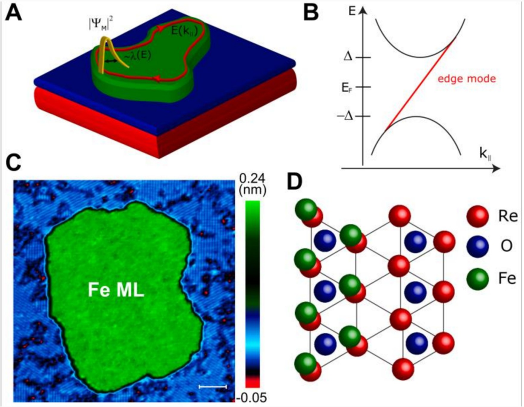

Chern number

C = 20

A. Palacio-Morales, ... & R. Wiesendanger, Science Adv. 5, eaav6600 (2019).

University of Hamburg (Germany)

VAN DER WAALS HETEROSTRUCTURES

Ferromagnetic island $CrBr_3$ deposited on superconducting $NbSe_2$

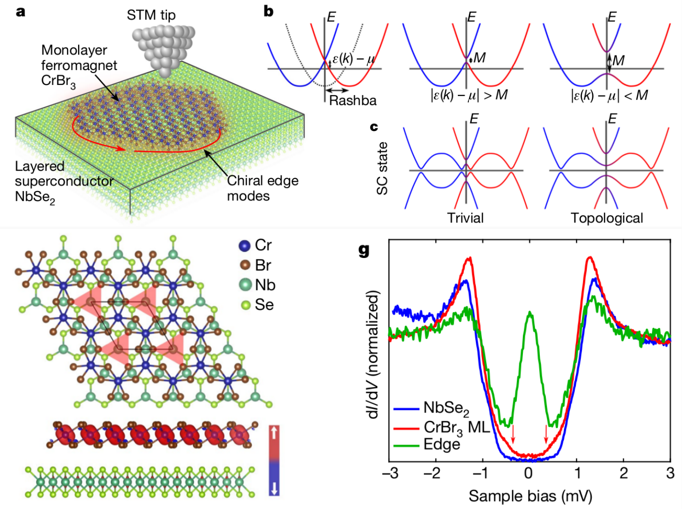

S. Kezilebieke ... Sz. Głodzik ... P. Lilienroth, Nature 424, 588 (2020).

MAGNETIC SKYRMION-TYPE TEXTURES

Scenario for topological superconductivity induced in 2D magnetic thin film hosting a skyrmion deposited on conventional s-wave superconductor

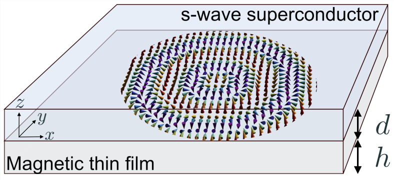

Scenario for topological superconductivity induced in 2D magnetic thin film hosting a skyrmion deposited on conventional s-wave superconductor

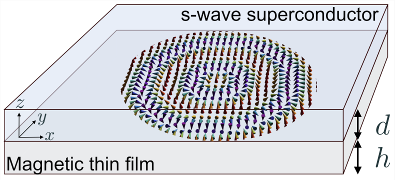

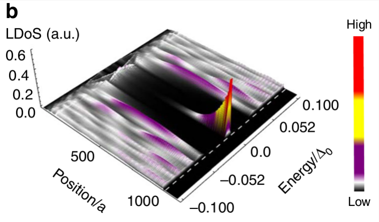

M. Garnier, A. Mesaros, P. Simon, Comm. Phys. 2, 126 (2019).

TOPOLOGICAL SUPERCOND. IN SKYRMION LATTICES

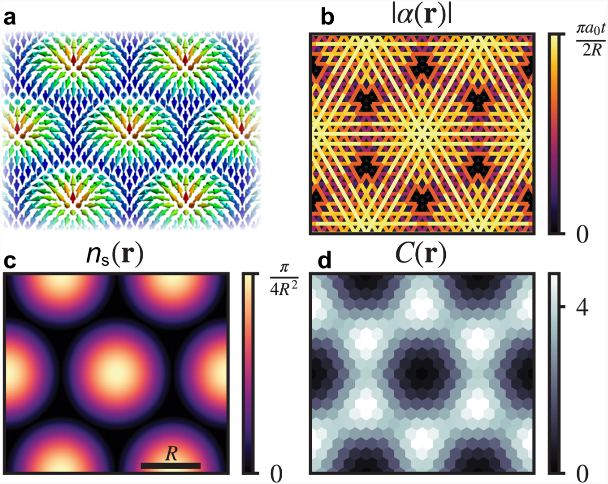

n_s - skyrmion number density

α - Rashba interaction

C - Chern number

E. Mascot, J. Bedow, M. Graham, S. Rachel, D.K. Morr, npj Quantum Mat. 6 (2021).

FINAL CONCLUSIONS

Magnetism and superconductivity

FINAL CONCLUSIONS

Magnetism and superconductivity

$\Longrightarrow$ **can constructively cooperate**

FINAL CONCLUSIONS

Magnetism and superconductivity

$\Rightarrow$ **can constructively cooperate**

$\Rightarrow$ **inducing novel (topological) states of matter**

FINAL CONCLUSIONS

Magnetism and superconductivity

$\Rightarrow$ **can constructively cooperate**

$\Rightarrow$ **inducing novel (topological) states of matter**

$\Rightarrow$ **hosting the exotic boundary modes**

FINAL CONCLUSIONS

Magnetism and superconductivity

$\Rightarrow$ **can constructively cooperate**

$\Rightarrow$ **inducing novel (topological) states of matter**

$\Rightarrow$ **hosting the exotic boundary modes**

$\Rightarrow$ **which are promising for quantum computing**